



New EWMA S^2 control charts for monitoring of process dispersion

M.R. Abujiya^a, M.H. Lee^{b,*} and M. Riaz^c

a. Department of Preparatory Year Program, King Fahd University of Petroleum and Minerals, Dhahran 31261, Saudi Arabia.
 b. Department of Mathematical Sciences, Faculty of Science, Universiti Teknologi Malaysia, 81310 UTM Skudai, Johor, Malaysia.
 c. Department of Mathematics and Statistics, King Fahd University of Petroleum and Minerals, Dhahran 31261, Saudi Arabia.

Received 23 July 2015; received in revised form 7 December 2015; accepted 9 February 2016

KEYWORDS

Average run length;
 Exponentially
 weighted moving
 average;
 Process dispersion;
 Ranked set sampling;
 Statistical process
 control.

Abstract. The Exponentially Weighted Moving Average (EWMA) control chart is an effective tool for the detection of small shifts in the process variability. This research studied the properties of EWMA charts based on unbiased sample variance, S^2 , for monitoring of changes in the process dispersion. However, since an increase in process variance could lead to an increased number of defective products, we only considered upward shifts in the process variance. The proposed schemes were based on simple random sampling and extreme variations of ranked set sampling technique for efficient monitoring. Using Monte Carlo simulations, we compared the relative performance of EWMA charts based on unbiased sample variance, S^2 , and its logarithmic transformation $\ln(S^2)$ as well as some existing schemes for monitoring the increases in variability of a normal process. It is found that the proposed schemes significantly outperform several other procedures for detecting increases in the process dispersion. Numerical example is given to illustrate the practical application of the proposed schemes using real industrial data.

© 2017 Sharif University of Technology. All rights reserved.

1. Introduction

The Exponentially Weighted Moving Average (EWMA) control chart, introduced by Roberts [1] for monitoring the process mean, has gained wide acceptance among practitioners due to its simplicity and effectiveness. The scheme has also found its way into detecting changes in process variability. Since the pioneering work of Wortham and Ringer [2], several enhancements of EWMA dispersion chart have been suggested. Crowder and Hamilton [3] proposed an EWMA control chart based on the natural logarithmic transformation of the ratio of sample variance S^2 to the in-control process variance σ_0^2 , $\ln(S^2/\sigma_0^2)$, for monitoring of the increases in the process variance. Their design structure resets the EWMA statistic to

zero whenever it falls below zero. Shu and Jiang [4], on the other hand, proposed resetting the EWMA dispersion chart by truncating the term $\ln(S^2/\sigma_0^2)$ to its approximate target value, which is the in-control mean of $\ln(S^2/\sigma_0^2)$, whenever it is less than the target.

More recently, Huwang et al. [5] proposed two EWMA control charts for monitoring the process variance. The two schemes were one-sided and designed to detect increases and decreases in process variability, respectively. Haq [6] suggested an improved mean deviation EWMA control chart [7] based on Ranked Set Sampling (RSS). Furthermore, Haq et al. [8-10] proposed new EWMA control charts for monitoring changes in the variance of a normally distributed process based on the Best Linear Unbiased Estimators (BLUE). The design structure of these schemes uses the RSS, Ordered RSS (ORSS), and Ordered Double RSS (ODRSS), respectively. RSS is a well-structured statistical technique for data collection that

*. Corresponding author.
 E-mail address: mhl@utm.my (M.H. Lee)

is more efficient than SRS in applications where the actual measurements of quality characteristics of interest may be costly, destructive, or time-consuming but they could be ranked by visual inspection or some inexpensive method without actual measurements [11,12].

Although the RSS scheme was, firstly, proposed for estimating mean pasture and forage yields in agriculture, the technique now has applications in many areas such as environmental and ecological studies [13,14], reliability theory [15], medical studies [16], marketing survey [17], and statistical quality control [18–20], to name but few. For more on recent applications and theoretical developments of RSS, see Wolfe [21], Al-Omari and Bouza [22], and references therein. Literature has shown that further gain in the efficiency of RSS is achievable when an appropriate unequal allocation of ranked units is used instead of equal allocation.

In practice, the highly recommended statistics for monitoring changes in the process dispersion are S^2 and its logarithmic transformation, $\ln(S^2)$ [4]. In this article, we propose new EWMA S^2 control charts for monitoring the variance of a process based on the extreme variations of RSS, namely, Extreme RSS (ERSS) [23] and Double Extreme RSS (DERSS) [24] sampling techniques.

The rest of the article is organized as follows: In the next section, we briefly introduce the design structure of the classical EWMA S^2 control chart. In Section 3, we present the design structure and statistical performance of the proposed EWMA S^2 charts based on the extreme variations of RSS. In Section 4, a comprehensive numerical comparison of the newly developed control schemes with some earlier EWMA charts for monitoring changes in the process dispersion are provided. Section 5 presents application examples of the proposed scheme using a real industrial data set and, finally, Section 6 provides the concluding remarks.

2. Classical EWMA S^2 control chart

To design the classical EWMA S^2 control chart based on SRS, let $X_{1,t}, X_{2,t}, X_{3,t}, \dots, X_{n,t}$, $t = 1, 2, 3, \dots$ be n independent and identically distributed normal $N(\mu_0, \sigma_0^2)$ random samples in a subgroup number, t , where μ_0 and σ_0^2 are the in-control process mean and variance, respectively. In a dispersion control chart, the process is initially assumed to be in-control with mean μ_0 and variance σ_0^2 , and remains in-control until it goes out-of-control with a shift in the process variance from σ_0^2 to $\sigma_t^2 > \sigma_0^2$. Define $\tau_t = \sigma_t/\sigma_0$ to be the magnitude of shift and let S_{srst}^2 represent the sequence of sample variances based on $X_{1,t}, X_{2,t}, X_{3,t}, \dots, X_{n,t}$ and given by:

$$S_{srst}^2 = \frac{1}{n-1} \sum_{i=1}^n (X_{i,t} - \bar{X}_{srst})^2, \quad (1)$$

where $\bar{X}_{srst} = (1/n) \sum_{i=1}^n X_{i,t}$ is the sample mean of the t th subgroup of size n . Following Shu and Jiang [4], we only considered the case of monitoring upward drifts in process variance as it resulted in an increased number of defective items. Similar to Crowder and Hamilton [3] EWMA statistic for monitoring of increases in process variability, $Q_{srst} = \max[0, \lambda \ln(S_{srst}^2/\sigma_0^2) + (1-\lambda)Q_{srst-1}]$, a corresponding statistic based on S^2 is defined as:

$$\tilde{Q}_{srst} = \max[\sigma_0^2, \lambda(S_{srst}^2/\sigma_0^2) + (1-\lambda)\tilde{Q}_{srst-1}], \quad (2)$$

where $0 < \lambda \leq 1$ is a smoothing constant and $\tilde{Q}_{srso} = 0$ [4]. It is well known that S_{srst}^2/σ_0^2 follows a gamma distribution with shape and scale parameters $\alpha = (n-1)/2$ and $\beta = 2\tau_t^2/(n-1)$, respectively. Using the extended version of EWMA chart based on S_{srst}^2 and suggested by Shu and Jiang [4], we write:

$$C_{srso} = 0$$

$$C_{srst} = \lambda Z_{srst} + (1-\lambda)C_{srst-1}, \quad (3)$$

where $Z_{srst} = (W_{srst} - \mu_{W_{srst}|\tau_t=1})$ and $W_{srst} = \max[\sigma_0^2, (S_{srst}^2/\sigma_0^2)]$. Clearly, the variance of C_{srst} is time varying [25] and by continuous substitution of C_{srst-j} , $j = 1, 2, 3, \dots, t$, we obtain:

$$C_{srst} = \lambda \sum_{j=0}^{t-1} (1-\lambda)^j Z_{srst-j} + (1-\lambda)^t C_{srso}. \quad (4)$$

Observe that:

$$\text{var}(C_{srst}) = \sigma_{W_{srst}|\tau_t=1}^2 \lambda [1 - (1-\lambda)^{2t}] / (2-\lambda),$$

where $\sigma_{W_{srst}|\tau_t=1}^2$ is the in-control variance of W_{srst} . Thus, the new EWMA chart gives an out-of-control signal when C_{srst} exceeds the upper control limit:

$$\text{UCL} = L\sigma_{W_{srst}} \sqrt{\lambda [1 - (1-\lambda)^{2t}] / (2-\lambda)}, \quad (5)$$

where L is chosen to satisfy the process control needs.

The statistical performance of a control chart is often measured in terms of the Run Length (RL) properties, which include its average (ARL) and standard deviation (SDRL). ARL represents the average number of samples required to signal an out-of-control or issue a false alarm. Using Monte Carlo simulations through an algorithm developed in FORTRAN, RL properties of the new EWMA S^2 charts are computed based on the assumption that quality characteristics of interest are normally distributed with an in-control process mean, $\mu_0 = 0$, and standard deviation, $\sigma_0 = 1$, without loss of

Table 1. RL characteristics of the classical EWMA S^2 control chart ($n = 5$, $ARL_0 = 500$).

λ	L	RL	τ_t												AEQL
			1.0	1.1	1.2	1.3	1.4	1.5	1.6	1.7	1.8	1.9	2.0		
0.05	2.750	ARL	500.73	47.98	16.32	8.60	5.58	4.06	3.20	2.66	2.29	2.02	1.85	1.030	
		SDRL	517.53	46.88	14.89	7.53	4.71	3.25	2.46	1.94	1.60	1.34	1.17		
0.10	3.318	ARL	500.55	60.29	19.81	10.13	6.44	4.64	3.60	2.94	2.52	2.22	1.99	1.164	
		SDRL	503.55	58.51	17.84	8.60	5.22	3.63	2.71	2.14	1.75	1.49	1.27		
0.25	4.265	ARL	500.03	86.18	27.98	13.31	8.00	5.58	4.23	3.40	2.85	2.48	2.20	1.397	
		SDRL	499.31	85.18	26.47	11.87	6.71	4.43	3.23	2.50	2.02	1.68	1.44		
0.50	5.131	ARL	500.14	112.29	38.54	18.02	10.28	6.80	4.93	3.89	3.19	2.71	2.38	1.673	
		SDRL	498.54	110.99	37.83	17.05	9.33	5.89	4.06	3.09	2.40	1.97	1.64		
0.75	5.594	ARL	500.39	127.45	46.50	21.87	12.40	7.97	5.64	4.32	3.48	2.90	2.52	1.906	
		SDRL	497.92	126.69	46.12	21.21	11.78	7.30	4.99	3.65	2.81	2.25	1.88		
1.00 (Shewhart chart)	5.749	ARL	500.25	136.33	51.87	24.84	14.07	8.99	6.34	4.75	3.76	3.13	2.66	2.105	
		SDRL	SDRL	135.45	51.67	24.29	13.56	8.48	5.84	4.20	3.23	2.59	2.11		

generality. Simulations are conducted based on 100,000 iterations for different shift τ_t values using a subgroup size of $n = 5$. Setting $\lambda = 0.05, 0.1, 0.25, 0.5, 0.75$, and 1.0 , the value of L is chosen to achieve in-control ARL_0 of 500, and the results are tabulated in Table 1. Observe that when $\lambda = 1.0$, the EWMA coincides with the Shewhart control chart.

Furthermore, we have also presented, in Table 1, the estimated Average Extra Quadratic Loss (AEQL) of the new EWMA S^2 charts as an overall performance measure over the entire process variance shifts as no control chart will give a better performance than others for all shift values in terms of out-of-control ARL and SDRL alone [26,27]. AEQL is based on a loss function and is used to measure the overall effectiveness of a control chart. It is computed by solving the integral equation:

$$AEQL = \frac{1}{\tau_{t \max} - \tau_{t \min}} \int_{\tau_{t \min}}^{\tau_{t \max}} \tau_t^2 ARL(\tau_t) d\tau_t, \quad (6)$$

where $ARL(\tau_t)$ is the ARL value of a particular chart at shift τ_t , $\tau_{t \max}$, and $\tau_{t \min}$ are the upper and lower bounds of shifts in process variance, respectively. Smaller values of AEQL indicate the overall effectiveness of a control chart. The advantage of the above procedure is its simplicity and excellent performance in detecting upward shifts in the process variability. To further enhance the ability of the EWMA S^2 control chart to detect shifts more quickly, we propose the design structure based on ERSS and DERSS sampling techniques.

3. New EWMA S^2 charts under ERSS and DERSS

Application of RSS in a statistical quality control chart

for monitoring the process mean is gaining popularity among researchers. For example, see [19,20,28–32] among others. However, only recently has the technique found its way into monitoring of process dispersion [6,8,10,33–35]. Moreover, extreme variations of RSS are more effective in the estimation of process variance than the RSS if the underlying distribution is normal [36].

3.1. ERSS method

ERSS is an extreme variation of RSS that does not require complete ranking of units as it involves the measurement of the smallest or largest observations [23,37,38]. The scheme has practical advantages over the regular RSS in the sense that it is prone to fewer errors associated with ranking of units in a subgroup and much easier to apply in the field. The ERSS procedure is as follows:

- Identify n^2 samples from the target population;
- Randomly group these samples into n sets, each of size n units;
- Rank the units within each set with respect to a variable of interest by visual inspection or some less-expensive method;
- If the set size is even, select the smallest unit from the first $n/2$ sets and the largest unit from the other $n/2$ sets;
- If the set size is odd, select the smallest unit from the first $(n-1)/2$ sets and the largest unit from the other $(n-1)/2$ sets, and measure the median observation from the remaining set;
- This completes one cycle of ERSS data of size n . The procedure may be repeated m times to obtain a sample of nm units of ERSS data.

Let $X_{(i:e)t}$ for $i = 1, 2, \dots, n$, and $t = 1, 2, \dots, m$ denote the smallest i th ($i = 1, 2, \dots, k = n/2$) set and the largest i th ($i = k + 1, k + 2, \dots, n$) set for the t th cycle if the subgroup size n is even. For odd subgroup size n , use the same notation to denote the smallest of the i th ($i = 1, 2, \dots, l = (n - 1)/2$) set, the median of the i th ($i = (n + 1)/2$) set, and the largest of the i th ($i = l + 1, l + 2, \dots, n$) set. Then, the unbiased estimator of the population variance (cf. Sinha and Purkayastha [39] and Yu et al. [40]) for the t th cycle is given by:

$$S_{ersst}^2 = \frac{1}{n - 1 + v_n} \sum_{i=1}^n (X_{(i:e)t} - \bar{X}_{ersst})^2, \quad (7)$$

where $\bar{X}_{ersst} = (1/n) \sum_{i=1}^n X_{(i:e)t}$ is the mean estimator for the t th cycle; $v_n = (1/n) \sum_{i=1}^n v_{(i:e)}^2$ is a known correction constant that depends on sample size n ; and $v_{(i:e)} = (\mu_{(i:e)} - \mu) / \sigma$; see Yu et al. [40] for more detail.

Generally, the performance of RSS depends on the accuracy of ranking of units in a subgroup with respect to the quality characteristic of interest. But, since the identification of extreme values in a set is much easier than identifying the i th units, ERSS is prone to fewer ranking errors [23]. However, the technique may not be entirely free of errors associated with ranking of units in practical applications. In other words, human judgements and decisions on ranking may not always be accurate and, hence, have adverse effect on the efficiency of the ERSS estimators. This is called imperfect ranking. Assume that (X, Y) denotes a bivariate normal random variable and suppose the regression of X on Y is linear. Let X be the quality characteristic of interest that is difficult to rank and Y be the corresponding auxiliary variable that could readily be measured [37,38]; then, we have:

$$X = \mu_x + \rho_{xy}(\sigma_x/\sigma_y)(Y - \mu_y) + \varepsilon, \quad (8)$$

where μ_x , μ_y , σ_x , and σ_y are the population means and standard deviations of X and Y ; ρ_{xy} is the correlation between X and Y ; and ε is an error term, which is independent of the auxiliary variable Y . This error term has a mean of zero and variance $\sigma_x^2(1 - \rho_{xy}^2)$. Let $Y_{(i:e)t}$ for $i = 1, 2, \dots, n$ and $t = 1, 2, \dots, m$ denote the i th smallest and largest values in the t th cycle of Y based on perfect ranking of subgroup size n ; and $X_{[i:e]t}$ be the corresponding judgment ordering of X associated with $Y_{(i:e)t}$. Thus, the Imperfect ERSS (IERSS) based variance estimator can be written as:

$$S_{iersst}^2 = \frac{1}{n - 1 + v_n} \sum_{i=1}^n (X_{[i:e]t} - \bar{X}_{iersst})^2, \quad (9)$$

where $X_{[i:e]t} = \mu_x + \rho_{xy}(\sigma_x/\sigma_y)(Y_{(i:e)t} - \mu_y) + \varepsilon_{it}$; and $\bar{X}_{iersst} = (1/n) \sum_{i=1}^n X_{[i:e]t}$ is the estimator of mean based on IERSS for the t th cycle.

3.2. DERSS method

The performance of ERSS can be enhanced by double application of the scheme. DERSS methodology is more effective in the estimation of the population parameters than SRS, RSS, and ERSS [24,41]. The DERSS is a two-stage ERSS procedure described as follows:

- Identify n^3 samples from the target population;
- Randomly allocate these samples to n sets, each of size n^2 samples;
- Use the ERSS procedure on each set to obtain n units of ERSS data, each of size n ;
- Apply the ERSS procedure again in step (c) to obtain DERSS of size n ;
- Repeat the procedure m times to obtain a sample with nm units of DERSS data.

The corresponding unbiased estimator of the population variance S_{dersst}^2 , based on DERSS samples for the t th cycle, can be written as:

$$S_{dersst}^2 = \frac{1}{n - 1 + v_n} \sum_{i=1}^n (X_{(i:\tilde{e})t} - \bar{X}_{dersst})^2, \quad (10)$$

where $X_{(i:\tilde{e})t}$ and $\bar{X}_{dersst} = (1/n) \sum_{i=1}^n X_{(i:\tilde{e})t}$ denote the DERSS observations and mean estimators, respectively. $v_n = (1/n) \sum_{i=1}^n v_{(i:\tilde{e})}^2$ is a known correction constant [40]. The corresponding imperfect DERSS is defined as:

$$S_{idersst}^2 = \frac{1}{n - 1 + v_n} \sum_{i=1}^n (X_{[i:\tilde{e}]t} - \bar{X}_{idersst})^2,$$

where:

$$X_{[i:\tilde{e}]t} = \mu_x + \rho_{xy}(\sigma_x/\sigma_y)(Y_{(i:\tilde{e})t} - \mu_y) + \varepsilon_{it},$$

and:

$$\bar{X}_{idersst} = (1/n) \sum_{i=1}^n X_{[i:\tilde{e}]t},$$

is the mean estimator of IDERSS for the t th cycle.

3.3. The design of EWMA S^2 charts using ERSS and DERSS

For simplicity, denote both the variances of ERSS and DERSS by S_{Xtrmt}^2 . The design structure of the new EWMA S^2 charts under ERSS and DERSS for monitoring of increases in process variability is based on the statistic:

$$\begin{aligned} C_{Xtrm0} &= 0, \\ C_{Xtrmt} &= \lambda Z_{Xtrmt} + (1 - \lambda)C_{Xtrmt-1}, \end{aligned} \quad (11)$$

where $Z_{Xtrmt} = (W_{Xtrmt} - \mu_{W_{Xtrmt}|\tau_t=1}) / \sigma_{W_{Xtrmt}|\tau_t=1}$; $W_{Xtrmt} = \max[\sigma_0^2, (S_{Xtrmt}^2/\sigma_0^2)]$; and $\mu_{W_{Xtrmt}|\tau_t=1}$ is the in-control mean of W_{Xtrmt} . It is shown in the appendix that the variance of C_{Xtrmt} , based on ERSS, can be written as:

$$\text{var}(C_{Xtrmt}) = \sigma_{W_{Xtrmt}|\tau_t=1}^2 \lambda [1 - (1 - \lambda)^{2t}] / (2 - \lambda),$$

where $\sigma_{W_{Xtrmt}|\tau_t=1}^2$ is the in-control variance of W_{Xtrmt} . Both $\mu_{W_{Xtrmt}|\tau_t=1}$ and $\sigma_{W_{Xtrmt}|\tau_t=1}^2$ values were estimated using Monte Carlo simulations. The upper control limit of the proposed chart is given by:

$$\text{UCL} = L \sigma_{W_{Xtrmt}} \sqrt{\lambda [1 - (1 - \lambda)^{2t}] / (2 - \lambda)}, \quad (12)$$

and the scheme triggers an out-of-control signal whenever $C_{Xtrmt} > \text{UCL}$.

The statistical performance of the proposed schemes was evaluated using $n = 5$ and $\text{ARL}_0 = 200, 370, \text{ and } 500$. Without loss of generality, we assume the in-control observations to be from a standard normal distribution. Setting $\lambda = 0.05, 0.1, 0.25, 0.5, 0.75$, and 1.0 , the control limit, L , is adjusted to obtain the desired ARL_0 . Using Monte Carlo simulations, the RL properties of the proposed ERSS based charts are computed based on the following outlined steps, while those of other sampling schemes have similar fashions.

1. Generate pseudo random numbers, $X_{i,t}$, from a standard normal distribution;
2. Apply the ERSS procedure to $X_{i,t}$, estimate \bar{X}_{ersst} , and directly compute S_{ersst}^2 , Eq. (7);
3. Compute the ERSS based $\mu_{W_{Xtrmt}}$, $\sigma_{W_{Xtrmt}}$, and Z_{Xtrmt} in Subsection 3.3;
4. Initialize the control chart statistic, C_{Xtrmt0} , Eq. (11), equal to zero;

5. Set the control chart parameter, $0 < \lambda \leq 1$, and update the statistic C_{Xtrmt} , Eq. (11);
6. Calculate the experimental control limit UCL, Eq. (12), using experimental L values;
7. Compare the statistic C_{Xtrmt} with UCL and record run-length;
8. After 100,000 iterations, compute the Average Run-Length (ARL) and standard deviation (SDRL);
9. Repeat steps 6 to 8 until the desired ARL_0 is achieved.

The above design procedure is for the computation of ARL_0 when $\tau_t = 1$. To compute the out-of-control ARL for different shift $\tau_t > 1$ values, only steps 1 to 8 are required, since the UCL is pre-determined from the computation of ARL_0 . The results obtained based on ERSS and DERSS are presented in Tables 2 and 3. In this article, only the case of $\text{ARL}_0 = 500$ is reported for lack of space. For simplicity, the design structure based on ERSS and DERSS will hence be referred to as Schemes I and II, respectively, throughout the remainder of the article.

Examination of Tables 2 and 3 shows that both the out-of-control ARL and SDRL decrease rapidly as changes in the process dispersion increase, while the in-control SDRL values for both schemes are approximately same as the corresponding ARL_0 values. Furthermore, the out-of-control ARL and SDRL values indicate that the proposed schemes are particularly more effective in detecting small changes when the value of λ is small while a large value of λ is more sensitive to moderate and large changes in the variability of a process. In the overall performance, the proposed schemes have significantly minimized the AEQL values of the EWMA S^2 control chart. Moreover, the proposed Scheme II appeared to be the best choice as it

Table 2. RL characteristics of proposed Scheme I ($n = 5$, $\text{ARL}_0 = 500$).

λ	L	RL	τ_t												AEQL
			1.0	1.1	1.2	1.3	1.4	1.5	1.6	1.7	1.8	1.9	2.0		
0.05	2.702	ARL	500.36	28.35	9.22	4.90	3.25	2.44	1.98	1.70	1.51	1.38	1.29	0.650	
		SDRL	518.26	26.40	7.87	3.89	2.40	1.66	1.26	1.00	0.81	0.67	0.57		
0.10	3.228	ARL	500.26	35.50	10.95	5.69	3.69	2.72	2.17	1.84	1.62	1.47	1.35	0.716	
		SDRL	506.29	33.06	9.04	4.38	2.65	1.84	1.37	1.08	0.89	0.75	0.63		
0.25	4.067	ARL	500.77	52.57	14.79	7.04	4.38	3.13	2.45	2.04	1.77	1.57	1.44	0.824	
		SDRL	501.42	50.80	13.09	5.61	3.23	2.14	1.57	1.23	0.99	0.83	0.71		
0.50	4.819	ARL	500.22	74.91	21.26	9.22	5.27	3.57	2.71	2.19	1.87	1.65	1.49	0.949	
		SDRL	496.95	73.95	20.14	8.14	4.27	2.69	1.89	1.41	1.12	0.93	0.78		
0.75	5.227	ARL	500.21	91.23	27.24	11.70	6.36	4.10	2.98	2.35	1.95	1.70	1.52	1.071	
		SDRL	498.73	90.79	26.54	10.96	5.66	3.40	2.29	1.68	1.28	1.03	0.85		
1.00 (Shewhart chart)	5.366	ARL	500.09	101.69	32.42	13.92	7.46	4.71	3.30	2.54	2.06	1.76	1.57	1.190	
		SDRL	SDRL	101.28	31.89	13.45	6.94	4.18	2.76	1.98	1.47	1.16	0.94		

Table 3. RL characteristics of proposed Scheme II ($n = 5$, $ARL_0 = 500$).

λ	L	RL	τ_t												AEQL
			1.0	1.1	1.2	1.3	1.4	1.5	1.6	1.7	1.8	1.9	2.0		
0.05	2.689	ARL	500.05	17.92	5.76	3.12	2.14	1.67	1.41	1.25	1.16	1.10	1.06	0.473	
		SDRL	518.94	15.68	4.53	2.18	1.33	0.92	0.67	0.51	0.40	0.31	0.25		
0.10	3.198	ARL	500.02	22.24	6.74	3.57	2.39	1.83	1.51	1.33	1.21	1.13	1.08	0.508	
		SDRL	505.24	19.44	5.11	2.43	1.46	1.02	0.75	0.58	0.45	0.36	0.29		
0.25	3.999	ARL	500.05	33.32	8.72	4.25	2.75	2.04	1.66	1.42	1.27	1.18	1.12	0.563	
		SDRL	503.74	31.31	6.98	2.96	1.72	1.16	0.85	0.66	0.52	0.42	0.34		
0.50	4.711	ARL	500.52	51.23	12.38	5.33	3.15	2.23	1.75	1.48	1.31	1.21	1.13	0.629	
		SDRL	500.59	50.58	11.08	4.25	2.20	1.38	0.97	0.73	0.57	0.46	0.36		
0.75	5.094	ARL	500.53	66.48	16.89	6.73	3.64	2.45	1.84	1.52	1.33	1.21	1.14	0.695	
		SDRL	498.75	65.79	16.11	5.96	2.90	1.74	1.15	0.82	0.62	0.48	0.38		
1.00 (Shewhart chart)	5.228	ARL	500.50	77.83	21.03	8.36	4.35	2.71	1.97	1.58	1.35	1.22	1.14	0.765	
		SDRL	SDRL	77.05	20.48	7.79	3.85	2.15	1.38	0.96	0.69	0.51	0.39		

exhibited better overall performance, in terms of ARL, SDRL, and AEQL, than the proposed Scheme I and classical chart.

4. Comparative studies

In this section, we compare the performance of the proposed schemes with that of six other EWMA control charts for monitoring the process variability. Using $n = 5$, we set $ARL_0 = 200$ for a fair comparison. All the control charts are designed to detect small ($\lambda = 0.05$) and moderate ($\lambda = 0.3$) increases in the process dispersion based on the assumption that the underlying distribution is normal with a constant process mean. The performance of each control chart is evaluated in terms of ARL and overall performance measures, AEQL, Average Ratio of ARL (ARARL), and Performance Comparison Index (PCI). The ARARL is an integral equation that measures the overall effectiveness of a control chart across a range of shifts [42]. It is defined by:

$$ARARL = \frac{1}{\tau_{t \max} - \tau_{t \min}} \int_{\tau_{t \min}}^{\tau_{t \max}} \frac{ARL(\tau_t)}{ARL(\tau_t)_{\text{benchmark}}} d\tau_t, \quad (13)$$

where $\tau_{t \max}$ and $\tau_{t \min}$ are the maximum and minimum shifts; and $ARL(\tau_t)$ and $ARL(\tau_t)_{\text{benchmark}}$ are the ARL values of particular and benchmark control charts, respectively. Benchmark chart is one with the smallest out-of-control ARL. The PCI, on the other hand, is the ratio of the AEQL of a particular chart to AEQL of the best-performing control chart [43]:

$$PCI = AEQL / AEQL_{\text{benchmark}}. \quad (14)$$

The ARL values based on 100,000 iterations as well as the ARARL, AQEL, and PCI values are presented in

Tables 4 and 5, ordered from left to right based on their detection ability. The smaller the ARARL, AQEL, and PCI values, the better the performance of the scheme.

4.1. CH-EWMA control chart (Crowder and Hamilton, 1992)

The CH-EWMA chart by Crowder and Hamilton [3] is the first scheme to use the normal approximation of (S^2/σ_0^2) for monitoring upward shifts in the process dispersion. The ARL values for the CH-EWMA chart based on time-varying control limits are given in column 1 of both Tables 4 and 5. Comparison indicates that the proposed schemes have smaller ARL values than the CH-EWMA chart. In fact, the ARL values of Scheme II are less than half those of the CH-EWMA chart. Furthermore, the overall performance in terms of AEQL, ARARL, and PCI reveals that the CH-EWMA control chart is substantially less effective than all the proposed schemes. Based on their positions in Tables 4 and 5, CH-EWMA chart is the weakest performing scheme in detecting increases in process variability.

4.2. NEWMA control chart (Shu and Jiang, 2008)

The New EWMA (NEWMA) chart by Shu and Jiang [4] is also based on the log transformation $\ln(S^2/\sigma_0^2)$ and is an improvement on CH-EWMA chart, particularly when small shifts are of interest. The scheme uses truncation method, which helps in quick detection of upward shifts in the process variability. The RL performance of the NEWMA chart in detecting increases in variance is presented in column 2 of both Tables 4 and 5. As expected, the corresponding NEWMA chart based on S^2/σ_0^2 in column 3 is slightly more efficient in detecting increases in the process dispersion for moderate to large shifts. Further comparison indicates

Table 4. ARL comparison among EWMA dispersion control charts for $\lambda = 0.05$ when $n = 5$ at $ARL_0 = 200$.

τ	CHEWMA	NEWMA	Classical IEWMA S^2	FNEWMA	RSS EWMA	Scheme I	ODRSS EWMA	Scheme II
	$L = 1.087$	$L = 1.992$	$L = 2.106$	$L = 2.093$	$L = 1.910$	$L = 2.085$	$L = 1.914$	$L = 2.083$
1.0	200.250	200.558	200.209	200.236	200.530	200.241	200.318	200.181
1.1	34.388	27.909	29.234	23.672	19.670	18.481	16.941	12.244
1.2	12.549	11.262	11.439	8.590	7.310	6.784	6.301	4.390
1.3	6.803	6.510	6.432	4.675	4.220	3.848	3.639	2.524
1.4	4.612	4.507	4.350	3.149	2.970	2.671	2.569	1.824
1.5	3.517	3.447	3.285	2.407	2.250	2.075	2.011	1.472
1.6	2.854	2.818	2.669	1.982	1.870	1.730	1.660	1.278
1.7	2.437	2.396	2.249	1.724	1.642	1.511	1.482	1.166
1.8	2.147	2.108	1.985	1.559	1.468	1.374	1.338	1.104
1.9	1.934	1.900	1.784	1.440	1.350	1.277	1.240	1.061
2.0	1.776	1.742	1.646	1.353	1.280	1.210	1.170	1.037
AEQL	0.913	0.885	0.845	0.651	0.606	0.563	0.543	0.430
PCI	2.121	2.056	1.964	1.512	1.408	1.309	1.263	1.000
ARARL	2.273	2.154	2.095	1.605	1.469	1.363	1.305	1.000

Table 5. ARL comparison among EWMA dispersion control charts for $\lambda = 0.30$ when $n = 5$ at $ARL_0 = 200$.

τ	CHEWMA	NEWMA	Classical IEWMA S^2	FNEWMA	RSS EWMA	Scheme I	ODRSS EWMA	Scheme II
	$L = 1.600$	$L = 2.887$	$L = 3.666$	$L = 2.591$	$L = 2.971$	$L = 3.527$	$L = 2.612$	$L = 3.480$
1.0	200.694	200.104	200.156	200.127	200.284	200.190	200.112	200.095
1.1	48.262	43.157	47.961	32.300	34.428	32.050	28.889	21.890
1.2	19.034	16.825	18.656	11.370	11.487	10.923	10.021	6.853
1.3	10.297	9.260	9.877	6.130	5.669	5.627	5.309	3.577
1.4	6.754	6.147	6.350	4.080	3.660	3.672	3.501	2.378
1.5	4.992	4.554	4.583	2.970	2.720	2.713	2.633	1.816
1.6	3.929	3.642	3.578	2.380	2.211	2.169	2.097	1.510
1.7	3.281	3.050	2.942	2.040	1.902	1.826	1.802	1.315
1.8	2.816	2.643	2.509	1.778	1.692	1.616	1.602	1.203
1.9	2.503	2.337	2.210	1.590	1.553	1.460	1.429	1.130
2.0	2.259	2.114	1.979	1.480	1.440	1.346	1.329	1.082
AEQL	1.248	1.151	1.139	0.775	0.737	0.709	0.687	0.506
PCI	2.465	2.272	2.250	1.530	1.455	1.401	1.357	1.000
ARARL	2.465	2.258	2.293	1.540	1.473	1.425	1.366	1.000

that the proposed Schemes I and II have smaller ARL values than the NEWMA chart. In the overall performance, both the proposed schemes dominate the NEWMA chart. For example, Scheme I outperformed NEWMA by over 57% in detecting increases in the process dispersion.

4.3. FNEWMA control chart (Abbasi and Miller, 2011a)

Using the Fast Initial Response (FIR) feature of [44], Abbasi and Miller [25] analyzed the performance of the

FIR NEWMA (FNEWMA) chart and revealed that the scheme was more sensitive than the NEWMA chart in monitoring increases in process variance. The addition of FIR feature significantly enhanced the sensitivity of the NEWMA chart. Based on the RL properties of the FNEWMA chart presented in columns 4 and 5 of Tables 4 and 5, respectively, the scheme has smaller ARL values than the classical EWMA S^2 chart, but larger ARL values than the proposed Schemes I and II. Furthermore, AEQL, ARARL, and PCI indicate that the proposed Schemes I and II are more powerful than

the FNEWMA chart in the detection of changes in process variability. The performance, however, decreases with an increase in value of the smoothing constant λ .

4.4. RSS EWMA S^2 chart (Haq et al., 2014a)

Haq et al. [8] proposed two EWMA S^2 charts based on BLUE using SRS and RSS methods. They showed that ARL profiles of their schemes not only were smaller than those of CH-EWMA and NEWMA charts, but also uniformly outperformed the ARL values of HHW1-EWMA and HH2-EWMA control charts proposed by Huwang et al. [5]. In this comparison, we considered the best-performing RSS EWMA S^2 chart, whose RL profiles are tabulated in columns 4 and 5 of Tables 4 and 5, respectively. Expectedly, the scheme dominates CH-EWMA and NEWMA charts, but is not as effective as the FNEWMA chart for moderate to large values of λ (cf. Table 5). Results also indicate that the proposed Schemes I and II have smaller ARL values than the RSS EWMA chart. Moreover, the proposed Schemes I and II are not only more powerful than the BLUE based RSS EWMA control chart, but also much easier to compute and implement.

4.5. ODRSS EWMA S^2 chart (Haq et al., 2014b)

As an improvement on the first-stage RSS EWMA S^2 charts based on BLUE, Haq et al. [9] suggested a second-stage Ordered Double-RSS (ODRSS) EWMA S^2 control chart to monitor process departures from target mean and variance. The upper-sided RL characteristics of the ODRSS EWMA S^2 charts are presented in column 7 of Tables 4 and 5. Comparison indicates that the scheme has smaller ARL values than the CH-EWMA chart, NEWMA chart, Classical

EWMA S^2 chart, FNEWMA chart, RSS EWMA chart, and the proposed Scheme I. In other words, the scheme outperforms all other charts in the comparison, except the proposed Scheme II, which uniformly outperforms the former in detecting increases in the process dispersion. For example, the proposed Scheme II is superior to the ODRSS EWMA S^2 charts in detecting increases by at least 26.3% in terms of AEQL (cf. Table 4). The percentage performance increases as the value of λ increases.

4.6. The effect of wrong judgement ranking

It is well known that SRS and perfect ranking are special cases of imperfect ranking with correlation coefficients of $\rho_{xy} = 0$ and $\rho_{xy} = 1$, respectively. To investigate the effect of imperfect ranking on the performance of the proposed Schemes I and II, we compute the ARL profiles based on $n = 5$ using Monte Carlo simulations. Setting $ARL_0 = 200$ and $\rho_{xy} = 0.5, 0.75, 0.9$, the imperfect extreme samples were generated from a bivariate standard normal distribution. Using a graphical display of RL curves, we compare the performance of the imperfect charts with some existing schemes, namely, the CH-EWMA chart, classical EWMA S^2 chart, and NEWMA chart.

From Figure 1, one can observe that imperfect ranking does have effect on the proposed schemes, but does not adversely affect the efficiency of the estimators too. Clearly, the proposed schemes are not doing badly even in the presence of errors in ranking. This means that the extreme variations of RSS are more robust against imperfect ranking. Although Scheme I appeared to be struggling when $\rho_{xy} \leq 0.5$, it outperformed the CH-EWMA, classical EWMA S^2 , and NEWMA charts when $\rho_{xy} > 0.5$. Moreover, the

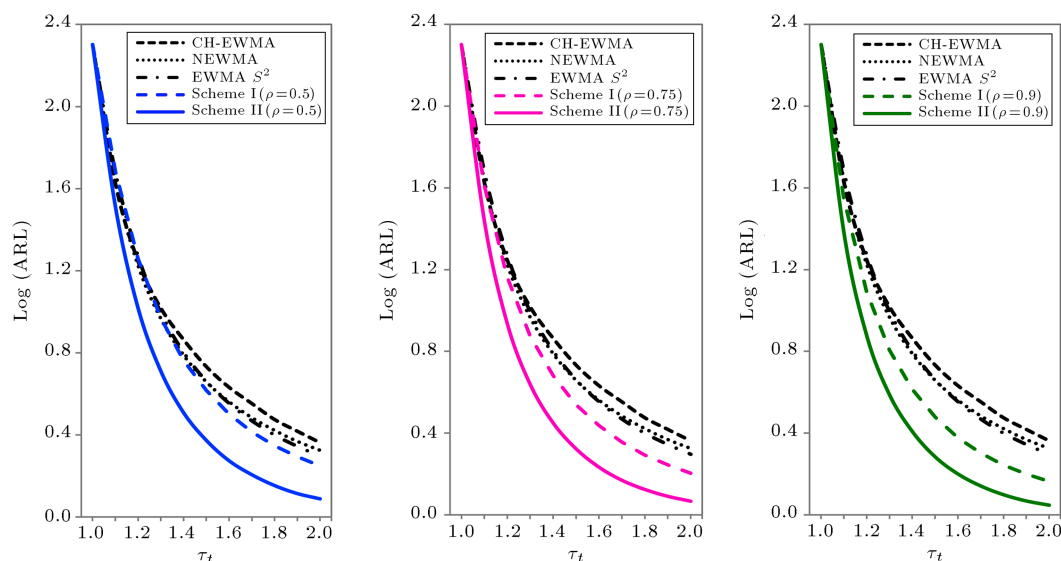


Figure 1. ARL curves for imperfect Schemes I and II versus CH-EWMA, NEWMA, and classical EWMA S^2 charts when $\lambda = 0.30$ and $n = 5$ at $ARL_0 = 200$.

proposed Scheme II uniformly outperformed all the other EWMA dispersion charts used in this comparative study.

5. Application example

This application is based on real data obtained from a filling bottle process in the production line of the Pepsi-Cola production company, Al-Khobar, Saudi Arabia, when the process is in-control [18]. The quality characteristic of interest is the quantity of liquid inside each bottle. The original data reasonably satisfy the normality assumption and, for our study purposes, we have standardized the whole data. Using the re-sampling approach of Takahasi and Wakimoto [12], 30 data points each of size $n = 5$ were randomly collected using SRS, ERSS, and DERSS methods. The design parameters for estimating the control limits and plotting statistics are based on $ARL_0 = 200$ and $\lambda = 0.3$. To measure how quickly the proposed schemes respond to upward shifts in variance, we introduce some noise by increasing each of the last 10 data points by 0.02 units. This means that the process is stable up to the 20th sample point before it goes out of control. The plotting statistics and control limits for the classical chart and Schemes I and II based on the contaminated data are displayed in Figures 2, 3, and 4, respectively.

In Figure 2, the classical EWMA r^{S^2} chart detects a random shift in the process dispersion at the 24th sample point and gives a total of 6 out-of-control points. The proposed Scheme I (cf. Figure 3), on the other hand, detects a random shift in the process at the 23rd sample point with a total of 7 out-of-control points at sample points 23, 25, 26, 27, 28, 29, and 30. In Figure 4, the proposed scheme has once again demonstrated its superiority over the classical scheme and Scheme I by detecting a random shift at the 22nd sample with a total of 8 out-of-control points. Thus, the proposed EWMA S^2 control charts can be used in practice as an effective alternative to the existing

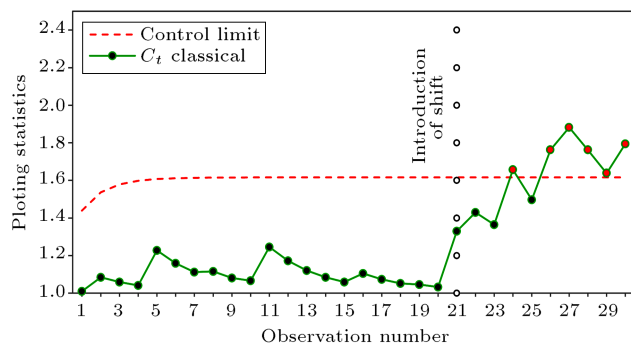


Figure 2. EWMA S^2 chart control chart based on classical scheme when $\lambda = 0.30$ and $n = 5$ at $ARL_0 = 200$.

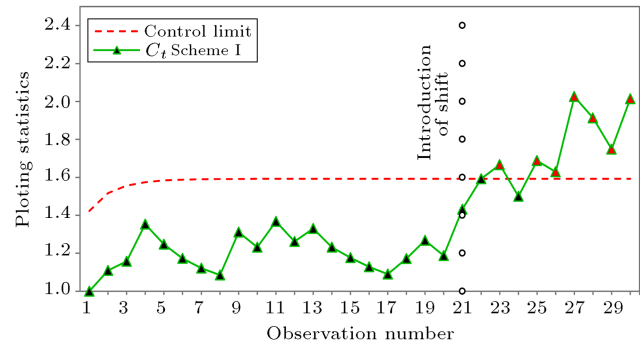


Figure 3. EWMA S^2 chart control chart based on Scheme I when $\lambda = 0.30$ and $n = 5$ at $ARL_0 = 200$.

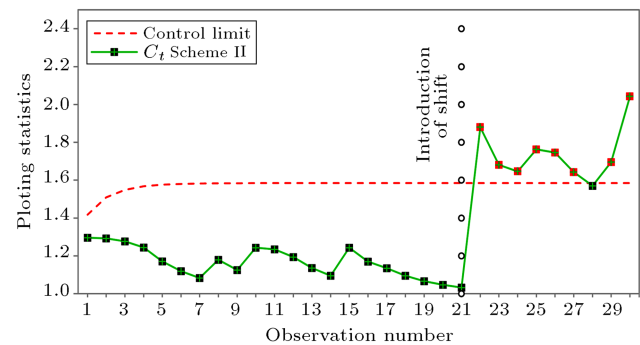


Figure 4. EWMA S^2 chart control chart based on Scheme II when $\lambda = 0.30$ and $n = 5$ at $ARL_0 = 200$.

EWMA schemes in detecting increases in the process dispersion.

6. Conclusions

This article proposes new EWMA S^2 chart statistics for effective monitoring of increases in the dispersion of a normal process. The performance of the classical EWMA S^2 charts was analyzed. To further increase the sensitivity of the charts to a wide range of upward shifts, two additional schemes based on the extreme variations of RSS were proposed. Monte Carlo simulation was used to estimate the RL properties of the new control charts. It is found that there are some improvements in the performance of the classical EWMA charts based on unbiased sample variance over its corresponding logarithmic transformation, $S^2 \ln(S^2)$. Furthermore, the proposed schemes based on the extreme variations of RSS outperform their existing counterparts in detecting positive shifts in the process variability.

The significance of the proposed schemes to monitor dispersion parameters has also been demonstrated through an application example. Hence, we recommend the use of the proposed EWMA schemes with even subgroup sizes by practitioners, since the identification of the smallest and largest observations is much easier than ranking all units in a subgroup. The

scope of this study may be extended to other control chart structures, particularly those based on EWMA operator, such as the adaptive cumulative sum and a variety of combined or mixed design schemes.

References

1. Roberts, S.W. "Control chart tests based on geometric moving averages", *Technometrics*, **1**(3), pp. 239-250 (1959).
2. Wortham, A.W. and Ringer, L.J. "Control via exponential smoothing", *The Logistics Review*, **7**(32), pp. 33-40 (1971).
3. Crowder, S.V. and Hamilton, M.D. "An EWMA for monitoring a process standard deviation", *Journal of Quality Technology*, **24**(1), pp. 12-21 (1992).
4. Shu, L. and Jiang, W. "A new EWMA chart for monitoring process dispersion", *Journal of Quality Technology*, **40**(3), pp. 319-331 (2008).
5. Huwang, L., Huang, C.-J. and Wang, Y.-H.T. "New EWMA control charts for monitoring process dispersion", *Computational Statistics & Data Analysis*, **54**(10), pp. 2328-2342 (2010).
6. Haq, A. "An improved mean deviation exponentially weighted moving average control chart to monitor process dispersion under ranked set sampling", *Journal of Statistical Computation and Simulation*, **84**(9), pp. 2011-2024 (2014).
7. Abbasi, S.A. and Miller, A. "MDEWMA chart: an efficient and robust alternative to monitor process dispersion", *Journal of Statistical Computation and Simulation*, **83**(2), pp. 247-268 (2011).
8. Haq, A., Brown, J. and Moltchanova, E. "New exponentially weighted moving average control charts for monitoring process dispersion", *Quality and Reliability Engineering International*, **30**(8), pp. 1311-1332 (2014).
9. Haq, A., Brown, J. and Moltchanova, E. "New exponentially weighted moving average control charts for monitoring process mean and process dispersion", *Quality and Reliability Engineering International*, **31**(5), pp. 877-901 (2015).
10. Haq, A., Brown, J., Moltchanova, E. and Al-Omari, A.I. "Improved exponentially weighted moving average control charts for monitoring process mean and dispersion", *Quality and Reliability Engineering International*, **31**(2), pp. 217-237 (2015).
11. McIntyre, G.A. "A method for unbiased selective sampling, using ranked sets", *Australian Journal of Agricultural Research*, **3**(4), pp. 385-390 (1952).
12. Takahasi, K. and Wakimoto, K. "On unbiased estimates of population mean based on sample stratified by means of ordering", *Annals of the Institute of Statistical Mathematics*, **20**(1), pp. 1-31 (1968).
13. Dell, T.R. and Clutter, J.L. "Ranked set sampling theory with order statistics background", *Biometrics*, **28**(2), pp. 545-553 (1972).
14. Al-Saleh, M.F. and Zheng, G. "Theory & methods: Estimation of bivariate characteristics using ranked set sampling", *Australian & New Zealand Journal of Statistics*, **44**(2), pp. 221-232 (2002).
15. Kvam, P.H. and Samaniego, F.J. "Nonparametric maximum likelihood estimation based on ranked set samples", *Journal of the American Statistical Association*, **89**(426), pp. 526-537 (1994).
16. Samawi, H.M. and Al-Sagheer, O.A.M. "On the estimation of the distribution function using extreme and median ranked set sampling", *Biometrical Journal*, **43**(3), pp. 357-373 (2001).
17. Kowalczyk, B. "Alternative sampling designs some applications of qualitative data in survey sampling", *Statistics in Transition*, **7**(2), pp. 427-443 (2005).
18. Muttlak, H.A. and Al-Sabah, W.S. "Statistical quality control based on ranked set sampling", *Journal of Applied Statistics*, **30**(9), pp. 1055-1078 (2003).
19. Mehmood, R., Riaz, M. and Does, R.J.M.M. "Control charts for location based on different sampling schemes", *Journal of Applied Statistics*, **40**(3), pp. 483-494 (2012).
20. Abujiya, M.R. and Muttlak, H.A. "Quality control chart for the mean using double ranked set sampling", *Journal of Applied Statistics*, **31**(10), pp. 1185-1201 (2004).
21. Wolfe, D.A. "Ranked set sampling: Its relevance and impact on statistical inference", *ISRN Probability and Statistics*, p. 32 (2012).
22. Al-Omari, A.I. and Bouza, C.N. "Review of ranked set sampling: modifications and applications", *Revista Investigación Operacional*, **35**(3), pp. 215-240 (2014).
23. Samawi, H.M., Ahmed, M.S. and Abu-Dayyeh, W. "Estimating the population mean using extreme ranked set sampling", *Biometrical Journal*, **38**(5), pp. 577-586 (1996).
24. Samawi, H.M. "On double extreme rank set sample with application to regression estimator", *Metron - International Journal of Statistics*, **60**(1-2), pp. 50-63 (2002).
25. Abbasi, S. and Miller, A. "Increasing the sensitivity of variability EWMA control charts", In *Electrical Engineering and Applied Computing*, Ao, S.I., and Gelman, L., Eds., pp. 431-443, Springer Netherlands (2011).
26. Reynolds, M.R. and Stoumbos, Z.G. "Comparisons of some exponentially weighted moving average control charts for monitoring the process mean and variance", *Technometrics*, **48**(4), pp. 550-567 (2006).
27. Wu, Z., Jiao, J., Yang, M., Liu, Y. and Wang, Z. "An enhanced adaptive CUSUM control chart", *IIE Transactions*, **41**(7), pp. 642-653 (2009).
28. Al-Sabah, W.S. "Cumulative sum statistical control charts using ranked set sampling data", *Pakistan Journal of Statistics*, **26**(2), pp. 365-378 (2010).

29. Jafari, J.M. and Mirkamali, S.J. "Control charts for attributes with maxima nominated samples", *Journal of Statistical Planning and Inference*, **141**(7), pp. 2386-2398 (2011).
30. Al-Omari, A.I. and Haq, A. "Improved quality control charts for monitoring the process mean, using double-ranked set sampling methods", *Journal of Applied Statistics*, **39**(4), pp. 745-763 (2012).
31. Haq, A. and Al-Omari, A. "A new Shewhart control chart for monitoring process mean based on partially ordered judgment subset sampling", *Qual. Quant.*, **49**(3), pp. 1185-1202 (2015).
32. Abujiya, M.R., Lee, M.H. and Riaz, M. "Improving the performance of exponentially weighted moving average control charts", *Quality and Reliability Engineering International*, **30**(4), pp. 571-590 (2014).
33. Abujiya, M.R., Lee, M.H. and Riaz, M. "Combined application of shewhart and cumulative sum R chart for monitoring process dispersion", *Quality and Reliability Engineering International*, **32**(1), pp. 51-67 (2014).
34. Mehmood, R., Riaz, M. and Does, R.J.M.M. "Quality quandaries: on the application of different ranked set sampling schemes", *Quality Engineering*, **26**(3), pp. 370-378 (2014).
35. Abujiya, M.a.R., Riaz, M. and Lee, M.H. "Enhanced cumulative sum charts for monitoring process dispersion", *PLoS ONE*, **10**(4), p. e0124520 (2015).
36. Shaibu, A.B. and Muttlak, H.A. "Estimating the parameters of the normal, exponential and gamma distributions using median and extreme ranked set samples", *STATISTICA*, **64**(1), pp. 75-98 (2004).
37. Stokes, S.L. "Inferences on the correlation coefficient in bivariate normal populations from ranked set samples", *Journal of the American Statistical Association*, **75**(372), pp. 989-995 (1980).
38. Al-Saleh, M.F. and Al-Ananbeh, A.M. "Estimation of the means of the bivariate normal using moving extreme ranked set sampling with concomitant variable", *Statistical Papers*, **48**(2), pp. 179-195 (2007).
39. Sinha, B.K. and Purkayastha, S. "On some aspects of ranked set sampling for estimation of normal and exponential parameters", *Strm*, **14**(3), pp. 223-240 (1996).
40. Yu, P.H., Lam, K. and Sinha, B. "Estimation of normal variance based on balanced and unbalanced ranked set samples", *Environmental and Ecological Statistics*, **6**(1), pp. 23-46 (1999).
41. Al-Omari, A.I. "Estimation of mean based on modified robust extreme ranked set sampling", *Journal of Statistical Computation and Simulation*, **81**(8), pp. 1055-1066 (2010).
42. Wu, Z., Yang, M., Jiang, W. and Khoo, M.B.C. "Optimization designs of the combined Shewhart-CUSUM control charts", *Computational Statistics and Data Analysis*, **53**(2), pp. 496-506 (2008).
43. Ou, Y., Wu, Z. and Tsung, F. "A comparison study of effectiveness and robustness of control charts for monitoring process mean", *International Journal of Production Economics*, **135**(1), pp. 479-490 (2012).
44. Steiner, S.H. "EWMA control charts with time-varying control limits and fast initial response", *Journal of Quality Technology*, **31**(1), pp. 75-86 (1999).

Appendix

From the ERSS based EWMA test statistic:

$$C_{ersst} = \lambda Z_{ersst} + (1 - \lambda)C_{ersst-1},$$

and by continuous substitution of $C_{ersst-j}$, $j = 1, 2, 3, \dots, t$, we can write:

$$\begin{aligned} C_{ersst} &= \lambda Z_{ersst} + \lambda(1 - \lambda)Z_{ersst-1} \\ &\quad + \lambda(1 - \lambda)^2 Z_{ersst-2} + \lambda(1 - \lambda)^3 Z_{ersst-3} \\ &\quad + \dots + \lambda(1 - \lambda)^{t-1} Z_{ersst} \\ &\quad + (1 - \lambda)^t C_{erss0} = \lambda \sum_{j=0}^{t-1} (1 - \lambda)^j Z_{ersst-j} \\ &\quad + (1 - \lambda)^t C_{erss0}. \end{aligned}$$

Taking the variance of both sides, we can write:

$$\begin{aligned} \text{var}(C_{ersst}) &= \text{var} \left[\lambda \sum_{j=0}^{t-1} (1 - \lambda)^j Z_{ersst-j} \right. \\ &\quad \left. + (1 - \lambda)^t C_{erss0} \right] = \lambda^2 \sum_{j=0}^{t-1} (1 - \lambda)^{2j} \\ &\quad \text{var}(Z_{ersst-j}) + (1 - \lambda)^{2t} \text{var}(C_{erss0}), \end{aligned}$$

and since $X_{i,t}$, $i = 1, 2, 3, \dots, n$ are independent normal random variables, we have:

$$\begin{aligned} \text{var}(C_{ersst}) &= \lambda^2 \left[1 - (1 - \lambda)^{2t} \right] \\ &\quad / \left(1 - (1 - \lambda)^2 \right) \sigma_{W_{ersst}|\tau_t=1}^2 \\ &= \sigma_{W_{ersst}|\tau_t=1}^2 \lambda \left[(1 - (1 - \lambda)^{2t}) \right] / (2 - \lambda), \end{aligned}$$

where $\sigma_{W_{ersst}|\tau_t=1}^2 = \text{var}(Z_{ersst-j})$ is the variance of $W_{ersst} = \max[\sigma_0^2, (S_{ersst}^2/\sigma_0^2)]$, when the process is in-control.

Biographies

Mu'azu Ramat Abujiya is a Lecturer in Prep-Year Mathematics Program at King Fahd University of Petroleum & Minerals, Dhahran, Saudi Arabia. He holds the BS, MS, and PhD in Mathematics from Bayero University Kano, King Fahd University of Petroleum & Minerals, and Universiti Teknologi Malaysia, respectively. His research interests are in the areas of statistical process control, ranked set sampling, order statistics, and e-learning systems.

Muhammad Hisyam Lee is a Professor of Statistics in the Department of Mathematical Sciences, Faculty of Sciences, Universiti Teknologi Malaysia. He served as Vice President of the Malaysia Institute of Statistics

between 2010 and 2014. Currently, he is serving as the Manager of Information Technology in the office of the Deputy Vice-Chancellor, Academic and International, UTM. His research interests include forecasting, time series analysis, geostatistics, quality control, educational assessment, and structural equation modeling.

Muhammad Riaz is an Associate Professor in the Department of Mathematics and Statistics, King Fahd University of Petroleum & Minerals, Dhahran, Saudi Arabia. He received his PhD degree in Statistics from the Institute of Business and Industrial Statistics, University of Amsterdam, the Netherlands. His research interests include statistical process control, non-parametric techniques, and experimental design.